Available online at www.sciencedirect.com

jmr&t Journal of Materials Research and Technology

journal homepage: www.elsevier.com/locate/jmrt

Original Article

Effects of surface roughness on the hydrophilic particles-air bubble attachment

Shaoqi Zhou [a], Xiangning Bu [a,***], Xuexia Wang [a], Chao Ni [a], Guangxi Ma [a,b,**], Yujin Sun [c], Guangyuan Xie [a], Muhammad Bilal [d], Muidh Alheshibri [e,f], Ahmad Hassanzadeh [g,h], Saeed Chehreh Chelgani [i,*]

[a] Key Laboratory of Coal Processing and Efficient Utilization (Ministry of Education), School of Chemical Engineering and Technology, China University of Mining and Technology, Xuzhou 221116, China
[b] School of Resources and Environmental Engineering, Shandong University of Technology, Zibo 255000, China
[c] College of Mining Engineering, Taiyuan University of Technology, Taiyuan, 030024, Shanxi, China
[d] Department of Mining Engineering, Balochistan University of Information Technology Engineering and Management Sciences (BUITEMS), Quetta, Pakistan
[e] Department of Basic Sciences, Deanship of Preparatory Year and Supporting Studies, Imam Abdulrahman Bin Faisal University, P.O. Box 1982, Dammam 31441, Saudi Arabia
[f] Basic & Applied Scientific Research Center, Imam Abdulrahman Bin Faisal University, P.O. Box 1982, Dammam 31441, Saudi Arabia
[g] Department of Geoscience and Petroleum, Faculty of Engineering, Norwegian University of Science and Technology, 7491 Trondheim, Norway
[h] Maelgwyn Mineral Services Ltd, Ty Maelgwyn, 1A Gower Road, Cathays, Cardiff, CF24 4PA, United Kingdom
[i] Minerals and Metallurgical Engineering, Department of Civil, Environmental and Natural Resources Engineering, Luleå University of Technology, SE-971 87 Luleå, Sweden

ARTICLE INFO

Article history:
Received 26 January 2022
Accepted 12 April 2022
Available online 16 April 2022

Keywords:
Roughness
Particle-bubble attachment
Nanobubbles
Hydrophilicity

ABSTRACT

Bubble-particle attachment is a key factor in various material processing such as wastewater treatment and flotation separation. Nanobubble's formation and its stability on hydrophobic surfaces with and without surfactants have been scientifically proven and extensively studied in various investigations. However, the influence of particle roughness on the hydrophilic particle-air bubble attachment, which could be completely different from hydrophobic particle-bubble attachment in the presence of nanobubbles, has not been addressed. For tackling this gap, the present work investigated the impact of nanobubbles on the roughed surfaces of glass bead particles. The temperature rise technique as a known method was used for micro/nanobubble size generation. The glass beads were modified by the commonly applied abrasion method to create different roughness magnitudes. The particle-bubble assessment results indicated that the particle roughness could potentially affect the bubble attachment of hydrophilic glass beads while the attachment area of smooth particles was almost zero. Outcomes also were revealed that the modified attachment rate constant increased from 0.1180 to 2.2802 s^{-1} with the increase of particle

* Corresponding author.
** Corresponding author.
*** Corresponding author.
E-mail addresses: xiangning.bu@foxmail.com, xiangning.bu@cumt.edu.cn (X. Bu), cumtmgx@126.com (G. Ma), saeed.chelgani@ltu.se (S.C. Chelgani).

https://doi.org/10.1016/j.jmrt.2022.04.062

surface roughness, indicating a shortening of attachment performance by enhancing the particle surface roughness. However, it was observed that the temperature rise method could improve the particle-bubble attachment only to a marginal extent.

1. Introduction

The attachment of solid particles in aqueous solutions to air bubbles (conventional size mostly in the millimeter range) is critical in various industrial processes, including wastewater treatment, mineral processing, and pharmaceuticals [1]. Particle attachment to air bubbles is determined by different factors, including particle and bubble sizes [2], their surface physicochemical properties [3–6], particle density [2], hydrodynamic parameters [7], and bubble surface mobility [8,9]. These factors further influence the force between particles and bubbles involving the van der Waals, electrostatic double-layer, and hydrophobic forces (only for hydrophobic particles) [10,11]. The predominant function of hydrophobic force facilitates the attachment of hydrophobic particles to air bubbles [12,13]. Nevertheless, some studies have revealed that hydrophilic solid particles can still attach to bubble surfaces without hydrophobic interaction [1,14,15]. Derjaguin and Landau [16] attributed hydrophilic particles captured by the bubble to long-range electrostatic attraction and named the process "contactless flotation". The attachment between particles and bubbles does not form three-phase contact through this process. Uddin, Li, Mirnezami and Finch [14] could enhance the attachment of hydrophilic particles to the bubbles by introducing surfactants, which changed the surface potential of bubbles [14]. Their findings opened the possibility of manipulating bubble charges to depress gangue minerals. Fan, Zhang, Li and Rowson [1] believed that the attachment of purified quartz particles to air bubbles in surfactant-free aqueous solutions may have occurred due to the hydrogen bondings. In addition, it was reported that the shape of hydrophilic particles also affected their attachment to the bubble surface [17]. Irregular glass beads had greater adhesion than spherical ones since the irregular glass beads could easily rupture the water film between the particle and bubble [18].

The effect of surface roughness on the interaction between particles and bubbles can be easily obtained using the recent advancement in photographic techniques. It was documented that nanoscale roughness positively affects the flotation recovery of magnesite (hydrophilic particles), and the adhesion force for air bubbles with hydrophilic surfaces could reduce with increasing roughness on the hydrophilic surfaces [19]. Notably, plates are frequently used to investigate the influence of roughness on the attachment of particle-bubble. However, Sygusch and Rudolph [20] proved that the morphology affects the hydrophobicity and wetting behavior, but contact angle results from glass slide measurements cannot be transferred directly to particle-bubble attachment results.

In addition to wettability, the existence of micro/nano-sized surface roughness may unavoidably cause implications such as nanobubbles' nucleation and effects on particle-bubble (conventional size) attachment [19]. It was demonstrated that nanobubbles could be formed on the hydrophobic surface [21,22]. Nanobubbles could also form on hydrophilic surfaces, and their generations could be linked to the particle surface roughness [23]. Wu, Zhang, Zhang, Li, Sun, Zhang, Li, and Hu [21] explored the effect of nanobubbles produced by the alcohol-water exchange on the adsorption of bovine serum albumin (BSA) on Mica. Their experimental results have clearly shown that the nanobubbles influenced the adsorption of BSA. Maheshwari, vanKruijsdijk, Sanyal and Harvey [23] quantified nanobubbles' nucleation and growth behavior as a function of surface roughness and surface reaction rate. Recently, adding nanobubbles to the involving conventional bubble processes has been extensively examined and discussed as a technique for increasing the probability of hydrophobic particle-conventional air bubbles attachment [24–27]. Moreover, some studies have also shown that the existence of nanobubbles will slightly lead to the increase of kaolin entrainment in the process of coal flotation [28]. Therefore, it is very important to study the attachment between hydrophilic particles and bubbles in the presence of nanobubbles. However, surprisingly the nucleation of nanobubbles on hydrophilic particles and their influences on the of particles to bubbles attachment remains unknown. This is of great significance for a comprehensive understanding of the mechanism of nanobubbles and roughness in the flotation process.

In this work, for filling the gap, as an innovative approach, the effect of nanobubbles (generated by temperature rise method) on the attachment between hydrophilic glass bead particles and conventional size bubbles was investigated. The attachment of glass beads with different roughness magnitudes on bubbles was quantitatively estimated. The synergistic effect of nanobubbles and surface roughness on the particle-bubble attachment was explored for further assessment. And finally, the results have been systematically discussed to highlight the role of surface nanobubbles and surface roughness in the particle-bubble attachment. Outcomes of this investigation could open a new window for understanding surface nanobubbles' impact on the attachment between bubbles and rough hydrophilic particles.

2. Materials and methods

2.1. Materials

Hydrophilic glass beads (Biospec, US), all with a diameter of 0.1 mm, were employed for the particle-bubble attachment experiments. The contact angle of glass beads was about 19–22°. The glass plate was provided by the same manufacturer was

used to characterize the contact angle of glass beads, and the contact angle is measured by sessile drop. A Powereach JC2000D1 contact angle measurement apparatus (Shanghai Zhongchen Digital Technic Apparatus Co., Ltd., Shanghai, China) was used for water contact angle measurements. The measurement procedure has been described by Bu et al. (2019) [3]. Silicon carbide particles (SiC) (Baowei Jewelry Ltd, China) were used as the grinding medium in various sizes to create several degrees of roughness. Fig. 1 demonstrates the shape and surface properties of four different sizes of SiC particles given by scanning electron microscopy (SEM). The mean size (d_{50}) of the SiC was 39.55, 16.69, 2.72, and 1.52 μm, respectively, which was measured by a laser particle size analyzer (GSL-1000, Liaoning instrument research institute Co., Ltd, China). A significant amount of ultrapure water was stored and employed for all experimental works, with a conductivity of around 18.2 MΩ cm.

2.2. *Roughness*

To create various roughness on the particles and isolate the effect of shape from roughness, two morphological modification procedures can be considered: etching glass particles using hydrofluoric acid solution [29] and abrasion method [30–32]. In this study, the abrasion method modified the roughness of glass bead particles [33]. 30 g of glass beads along with 30 g SiC with a variety of mean sizes and 10 g stainless-steel balls with 1 mm diameter were weighed and placed in a 1 L vertical nylon cylinder. Due to the small size of silicon carbide particles, to facilitate the abrasion mechanism and interaction of the glass bead particles with the SiC during grinding, stainless-steel balls were added to the mill. The sample's nylon was then sealed with a fresh-keeping film and placed on the counter roller stirring at 100 rpm for 3 h of grinding. Subsequently, wet screening with a mesh size of 0.074 mm was applied to separate the glass beads from the SiC particles. After that, the glass beads were ultrasonically (40 kHz) cleaned up in alcohol for 5 min to remove any possible remaining SiC particles from their surface. Finally, the samples were dried overnight in a vacuum drying oven with a temperature of 105 °C. Smooth glass beads and glass beads ground by SiC with the d_{50} of 39.55, 16.69, 2.72, and 1.52 μm were marked as GB0, GB1, GB2, GB3, and GB4, respectively. The particle size distribution obtained from the laser particle size analyzer of glass beads before and after roughness treatment is shown in Fig. 2. It can be seen from Fig. 2, the particle size distribution of glass beads has not changed.

SEM images of glass beads with different roughness levels were presented in Fig. 3. Non-treated glass bead surfaces are extremely smooth, whereas the surface of glass beads ground with SiC becomes rough, and the roughness enhances with increasing SiC size. Pits emerge on the surface of glass beads ground by SiC with the mean size of 39.55 or 16.69 μm, while the pits on the glass bead surface ground by 39.55 μm SiC. Although there are no significant pits on the surface of the glass beads ground by 2.72/1.52 μm SiC, there are numerous scratches. The density of scratches rises as the SiC size decreases. The surface roughness of glass beads ground by SiC was estimated approximately by the length × width of pits. For counting the size of pits, 30 photos were selected. 30 glass

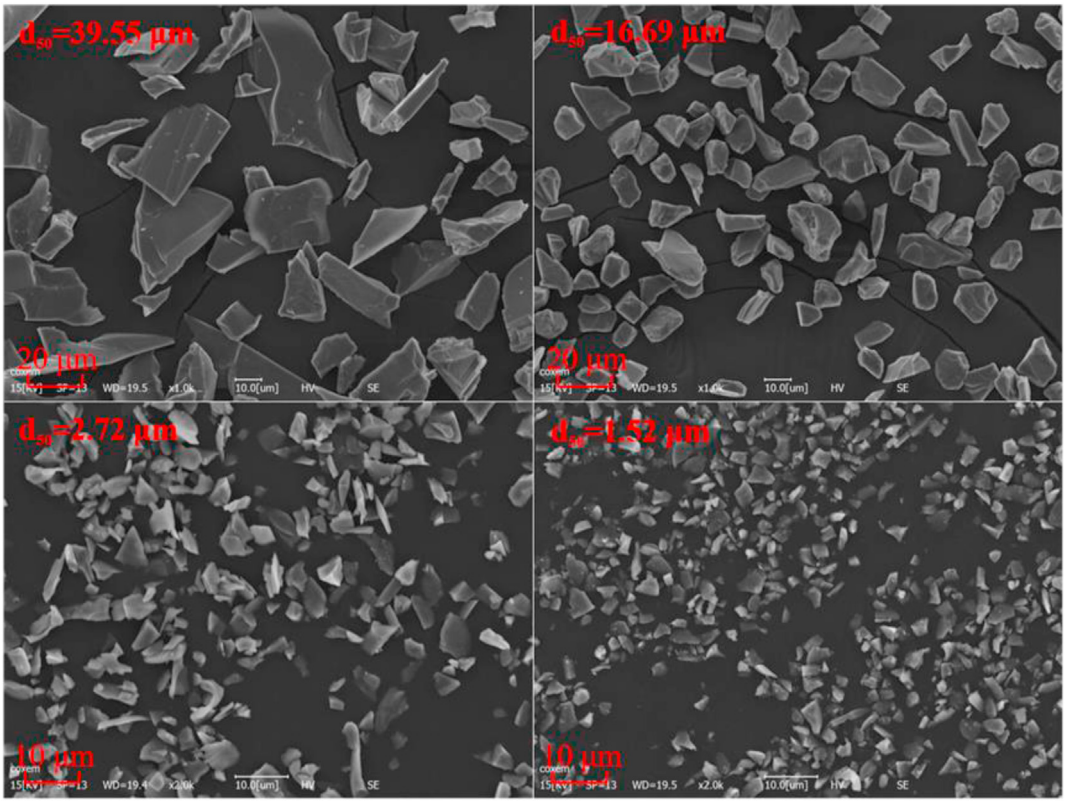

Fig. 1 – SEM images of silicon carbide particles for different size ranges.

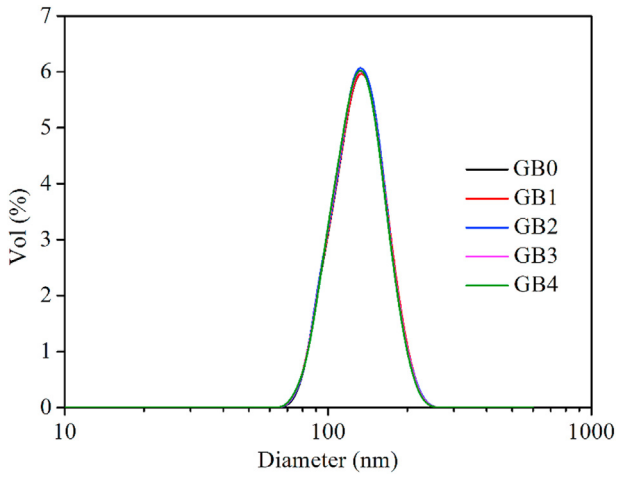

Fig. 2 – Particle size distribution of glass beads before and after roughness treatment.

beads in each photo were randomly selected for statistical assessments, and the pits on 900 particles under each condition were counted. The length × width of glass beads ground by SiC with the d_{50} of 39.55, 16.69, 2.72, and 1.52 μm were approximately 37.21 × 19.63, 19.86 × 7.53, 3.42 × 2.74, and 3.08 × 2.39 μm, respectively. In other words, the surface roughness of glass beads increased significantly by increasing the SiC size during the abrasion process of glass beads.

2.3. *Particle-bubble attachment tests*

An approach developed by Li et al. [34] was considered to assess the particle-bubble attachment. The experimental setup was primarily composed of the following components: i) a CCD camera, ii) a sample tank, iii) a magnetic stirrer, and iv) a syringe. The experimental processes of different solutions prior to particle-bubble attachment tests were shown schematically in Fig. 4. At the beginning of the conventional condition (Fig. 4-condition A), a blind attachment test was performed in ultrapure water at room temperature (25 °C). A sample tank containing 60 mL ultrapure water was filled with 1 g glass beads with a varied roughness degree. Glass beads were placed in water at room temperature and stirred for 40 min to serve as a control group (Fig. 4-condition B), and compared with the conventional condition (condition A of Fig. 4).

To investigate nanobubbles' effect on the bubble-glass beads attachment, two typical methods were considered, which have been commonly used to generate nanobubbles [35–37]. In the first method, ultrapure water was kept in airtight glass vials in the fridge at 4 °C for 72 h. Then, 1 g glass beads were dispersed in 60 mL cold water (4 °C) and stirred for 40 min with a magnetic stirrer, gradually bringing the suspension to room temperature (Fig. 4-condition C). Here the solubility of the dissolved gas is expected to be reduced and eventually nucleate nanobubbles. In addition, nanobubbles (Fig. 4-condition D) were produced by a nanobubbles generator (Langpai Technology Co., Ltd, Jinan, China), which was also used in the attachment test. The running time of the generator was 2 min, and the aeration rate was 0 mL/min. After preparing water containing numerous nanobubbles, it was allowed to stand for 10 min for testing. The concentration and size distribution of the bulk nanobubbles were measured by the nanoparticle tracking analysis (Nanosight-NS300, Malvern, the United Kingdom).

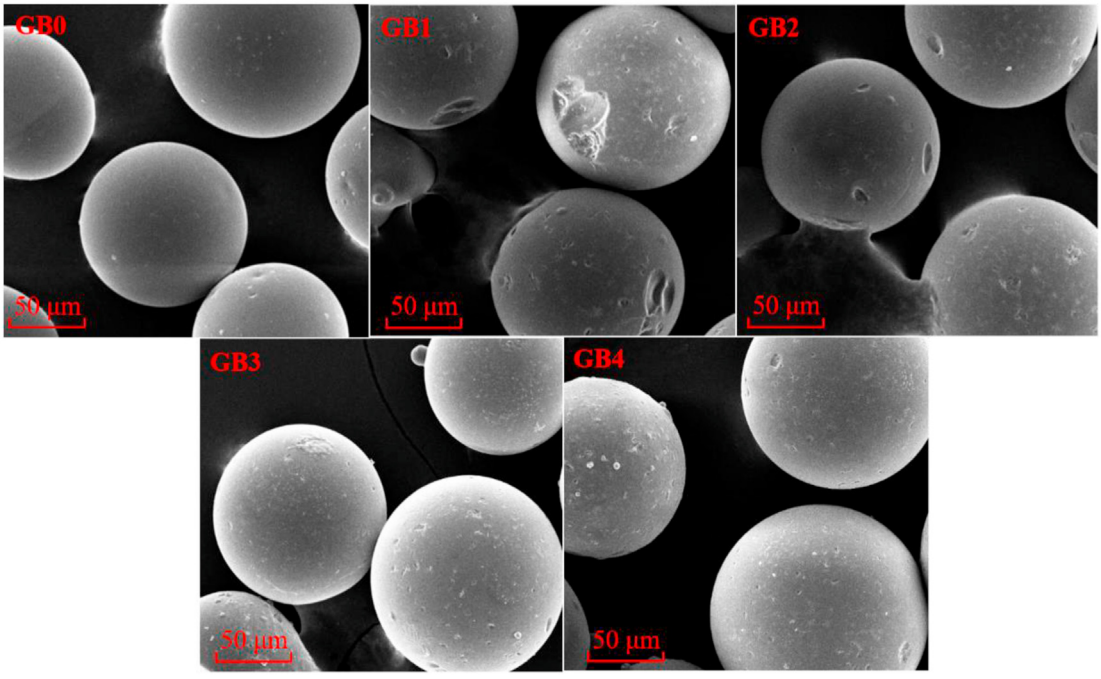

Fig. 3 – SEM photos of glass beads with different roughness magnitudes (smooth glass beads and ground ones by SiC with the d_{50} of 39.55, 16.69, 2.72, and 1.52 μm were marked as GB0, GB1, GB2, GB3, and GB4, respectively.).

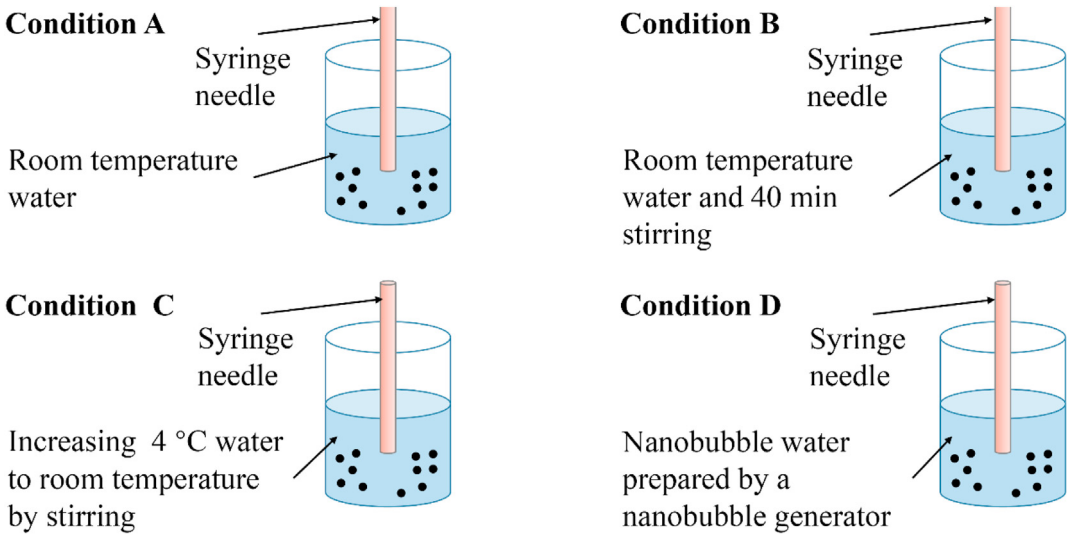

Fig. 4 – A schematic view of the experimental processes of different solutions prior to particle-bubble attachment tests.

Using a syringe, a 2.5 mm diameter air bubble was created at a depth of 30 mm below the water's surface. Such bubble diameter was selected to ease controlling the consistency of bubble sizes in each experiment. Detailed information regarding this procedure can be found elsewhere [34]. The magnetic stirrer was set at 500 rpm, and the CCD camera was used to capture the attachment of glass beads to the bubble surface after a specific attachment time (10, 30, 60, 90, and 180 s). Finally, the glass beads attached to the bubble surface were analyzed using Image J software. In each experiment, an image of bubble-particle attachment was taken to determine bubble-particle attachment area (A_a) (Fig. 5b). All tests were repeated three times, and the mean value was calculated following the Image J analysis software.

$$A_a = \pi L\left(R - \sqrt{R^2 - \left(\frac{L}{2}\right)^2}\right) \quad (1)$$

where A_a is the attachment area (the shadow region in Fig. 5b), L is the base length of the spherical crown, R is the bubble radius, and H is the height of the spherical crown.

3. Results and discussions

3.1. Attachment

Fig. 6 illustrates the area covered by smooth glass beads on the surface of bubbles in various pretreatment procedures. Based on these results, by increasing attachment time from 10 to 180 s, the area covered by smooth glass beads increased in all situations and reached a stable level at 180 s. Under condition C, the attachment rate of smooth glass bead particles on the bubble surface was remarkably faster than in the other conditions. The maximum A_a of 0.4 mm^2 was obtained when the attachment time was 60 s. However, under conditions A, B, and D, the A_a gently promoted by prolonging the attachment time. In other words, the A_a of smooth glass beads at condition C was the greatest (0.4 mm^2 at 60 s), followed by condition B (0.28 mm^2, 180 s), condition D (0.21 mm^2, 180 s), and the least was captured under condition A (0.1 mm^2, 180 s). A comparison between the rising temperature results, stirring for 40 min

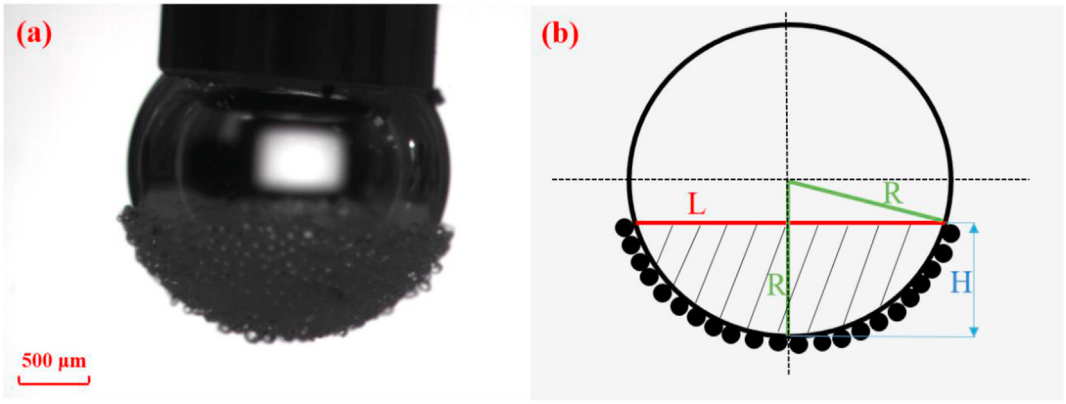

Fig. 5 – A schematic view of the bubble-particle attachment area determination: (a) image from the test, and (b) definition of A_a.

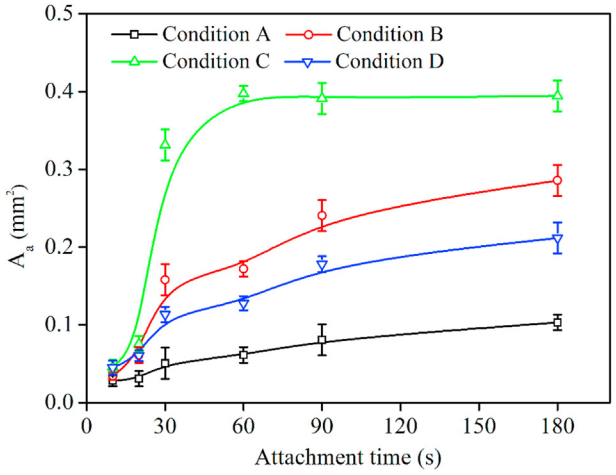

Fig. 6 – The A_a of smooth glass beads on the surface of bubbles after different pretreatment conditions (i.e., A: at room temperature water, B: room temperature water stirred for 40 min, C: water conditioned by the temperature rise method, and D: water contains nanobubbles).

(condition C), and the rest conditions indicated that the nanobubbles produced by the temperature rise method could potentially promote the attachment of smooth hydrophilic glass beads to the bubble surface. Another plausible reason could be attributed to the role of temperature on the adsorption rate of particles to the bubble surface.

3.2. *Roughness*

Evaluating A_a of glass beads with different roughness in condition A (Fig. 7) indicated that the A_a of smooth glass beads was varied from the rough surfaces. The A_a was almost constant for smooth surfaces and equaled approximately 0 (Fig. 7). However, the Aa was increased for rough glass beads when the surface roughness expanded under the same attachment time. The classical first-order model can characterize the kinetics of bubble-particle attachment and

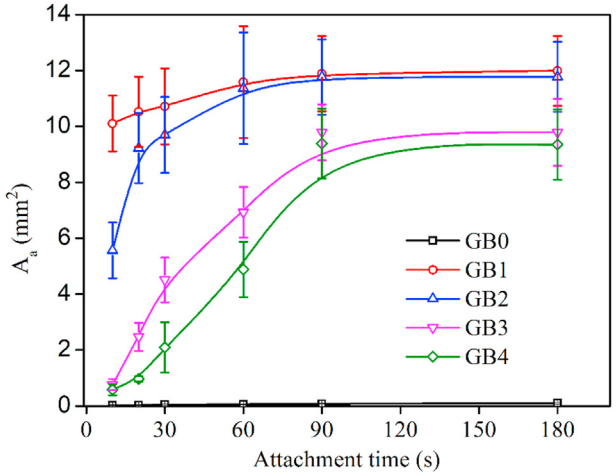

Fig. 7 – Estimated A_a for glass beads with different roughness on bubbles in the room temperature water (condition A).

detachment at a single-bubble scale [38]. To better evaluate the attachment behavior of particles with different roughness on bubbles, the first-order attachment equation ($A_a(t) = A_{a,\infty}(1\text{-}e^{-kx})$) was used to calculate the ultimate attachment area ($A_{a,\infty}$) and attachment rate constant (k, s^{-1}). This attachment equation could be referred to the classical first-order flotation kinetic model ($R(t) = R_\infty(1\text{-}e^{-kx})$) [39].

The evaluation outcomes (Table 1) demonstrated that the k of glass beads to bubbles surface was varied from 0.0096 to 0.1995 s^{-1} based on the various surface roughness. Rezai, Rahimi, Aslani, Eslamian, and Dehghani [40] reported improved flotation rate constant related to the roughness characteristics. Similar results were addressed by Guven, Celik, and Drelich [33], which confirmed a positive effect of particle surface roughness on quartz flotation kinetics and recoveries. The reported k values (Table 1) as a roughness function would be in line with the reported studies; however, the $A_{a,\infty}$ decreased with an increase in the surface roughness. The relatively small R^2 (the coefficient of determination) of 0.9124 somewhat indicated that the first-order attachment kinetics model is not applicable for such a system in some conditions. For such an assessment and fitting models for the flotation process, the R^2 value should be greater than 0.99 [41]. Moreover, different surface roughness resulted in variations of both $A_{a,\infty}$ and k; comparing the attachment kinetics under various surface roughness would be challenging. For flotation kinetics, numerous studies have used the modified attachment rate constant ($k_M = A_{a,\infty} \times k$) as an alternative for comparing the overall flotation responses under different conditions [42–47]. The value of k_M increased from 0.1180 to 2.2802 s^{-1} with the growth of particle surface roughness, indicating that the attachment performance would be shorter with the increase in the particle surface roughness.

The obtained A_a values (at 60 s attachment time) for the glass beads with different roughness (Fig. 8) showed that for smooth or rough glass bead particles, the presence of nanobubbles created by the temperature rise method slightly increased the A_a of glass beads on the bubble surface. This assessment released that the A_a of glass beads had the highest increase after pretreated by condition C at various roughness magnitudes. Although the A_a improved after being pretreated by condition B before the attachment test, the lifting was relatively smaller than the condition C. This phenomenon could most likely attribute to the fact that the nucleation of nanobubbles on the particle surface was more intensive after condition C than condition B. Since the water was only moderately stirred at room temperature under condition B, the gas nucleation probability caused by the low speed would be minimal. However, the temperature was adopted to

Table 1 – The classical first-order equation provided the outputs of non-linear regression fitting for various surface roughness of glass beads.

Sample	k (s^{-1})	$A_{a,\infty}$(%)	Adj.R^2	k_M (s^{-1})
GB1	0.1995	11.43	0.9830	2.2802
GB2	0.0677	11.69	0.9938	0.7917
GB3	0.0127	11.88	0.9604	0.2052
GB4	0.0096	12.24	0.9124	0.1180

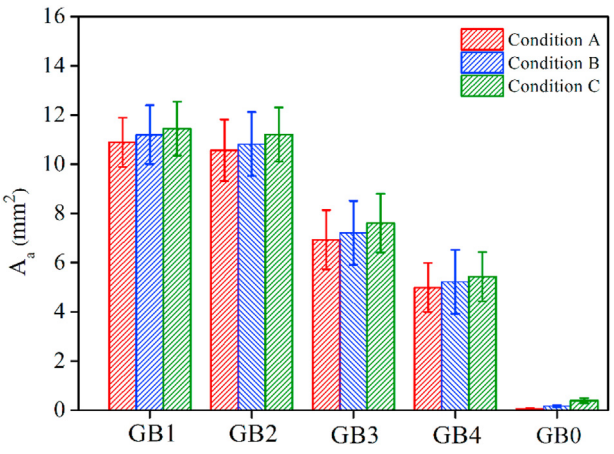

Fig. 8 – The A_a of glass beads with different roughness on the bubble surface under different studied conditions (the attachment time is 60 s).

condition C, in which the dissolved gas content of low-temperature water is significantly higher than that of room temperature water. During the heating process, releasing dissolved gas in cold water was induced gas nucleation, and its content was considerably more significant than the stirring condition. Additionally, roughness substantially affected the attachment of glass beads to the bubble surface (higher than it does on nanobubbles).

4. Discussion

The degree of attachment between air bubbles and hydrophobic particles would function the interaction energy governed by the dispersion, electrostatic double layer, and hydrophobic forces [15]. The hydrophilic particles-bubbles attachment could be different from and is mainly attributed to the long-range electrostatic attraction (contactless flotation) [1,14–16] and the presence of hydrogen bonds [48,49]. Due to the hydrophilic nature of particles, the particles and bubbles are most likely attracted to each other at the deep primary minimum of interaction potential without forming a three-phase contact line [15]. In the case of quartz, the attachment of purified particles to air bubbles in surfactant-free aqueous solutions was possibly due to hydrogen bond formation. The OH^- ions on air bubble surfaces formed hydrogen bonds with silicon and oxygen atoms in ≡Si–O–Si≡ or with the adsorbed OH group on quartz surfaces [1,48,49]. The formation of hydrogen bonds would increase by increasing contact area [1]. Furthermore, it was documented that when particles with specific kinetic energy collided with bubbles, their contact area affected the particle-bubble attachment [4]. Therefore, the hydrophilic particles-bubble attachment could also be significantly affected by the surface roughness of particles. The outcome of this investigation approved that by increasing hydrophilic particle surface roughness, their A_a on the bubble surface boosted gradually. It is well understood that by increasing roughness, the hydrophobicity of hydrophobic surfaces generally increases as well as the hydrophilicity of hydrophilic surfaces [50]. However, the wetting behavior of droplets on a rough plate would be entirely different from the attachment between bubbles and a smooth surface. For smooth glass beads (GB0), the contact area between particles and bubbles would be quite small and almost point contact (Fig. 9). In contrast, some pits on the particle surface of rough glass beads increased the contact area between particles and bubbles (GB1/GB2). This phenomenon indeed manifested that the contact area could improve by raising the surface roughness. By improving the contact area, the particles-bubble attachment could increase, which was intensified by forming the hydrogen bond.

Some investigations were reported that the temperature rise method could produce nanobubbles [37,51–53]. Furthermore, the mechanical stirring process has also been used to generate nanobubbles [15,54]. Experimental results also demonstrated that the presence of nanobubbles was likely to enhance the attachment of smooth hydrophilic glass beads to the bubble surface. Experiments with 40 min stirring treatment at room temperature (condition B) and room temperature rise method (condition C) could promote the attachment of smooth hydrophilic glass beads to the bubble surface compared to condition A. It was also observed that the A_a of particles with different roughness on the bubble surface improved in the presence of nanobubbles. However, nanobubbles showed a

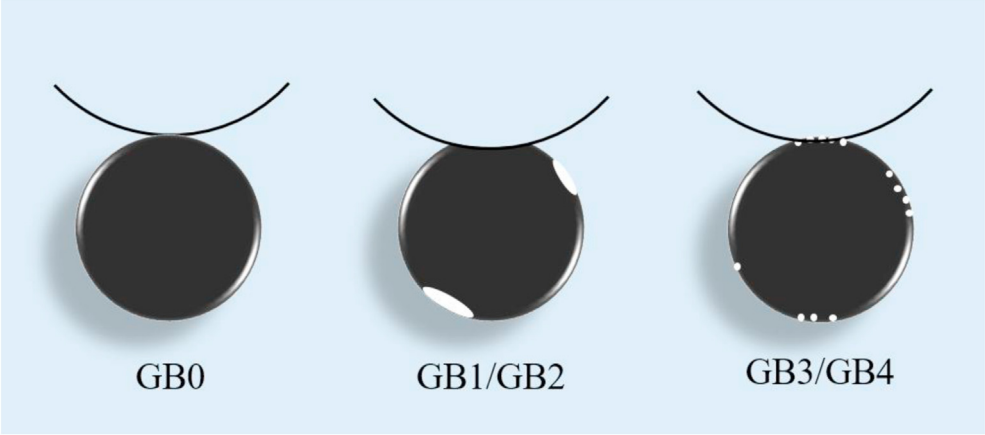

Fig. 9 – Schematic demonstration of particle roughness affecting particle-bubble attachment.

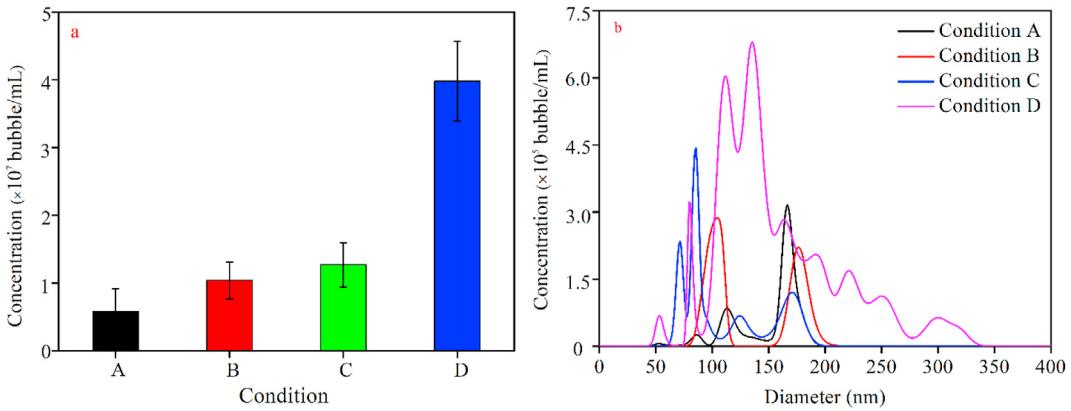

Fig. 10 – The (a) concentration and (b) size distribution of bulk nanobubbles at four different pretreatment conditions.

negligible effect on the attachment of hydrophilic glass beads to the bubbles compared to particles' roughness. It was reported that a nanoscale gas state could also occur on a smooth hydrophilic mica or silica surface. However, the population and volume of nanoscale gas state on hydrophilic surfaces are substantially smaller than that on hydrophobic surfaces. Because for hydrophilic surfaces, nanobubbles cannot exist stably, they can quickly spread and coalesce and form microbubbles, which eventually escape from the hydrophilic surfaces [21].

The A_a was much smaller when using commercial nanobubbles (condition D). To investigate this phenomenon, the concentration and size distribution of nanobubbles in the bulk phase were measured in each condition (Fig. 10). As shown in Fig. 10, the size distribution of bulk nanobubbles under different conditions is concentrated between 50 and 200 nm. But the size distribution range of nanobubbles under condition 4 is wider, and some bubbles with size in the range of 200–350 nm appear. This is because, under such high concentration, some nanobubbles will aggerate to form a nanobubble cluster [55]. Results illustrated that the bulk nanobubbles concentration in condition D is significantly higher than conditions B and C (Fig. 10). Although the concentration of bulk nanobubbles was low under condition C, condition C could produce several surface nanobubbles when the water contains glass beads. Wu, Wang, Harbottle, Masliyah, and Xu [15] reported a similar trend that the attachment of hydrophilic nanoparticles to sub-micron size bubbles might be enhanced by in-situ gas nucleation (surface nanobubbles). It could be induced by hydrodynamic cavitation for the weakly interacting systems, where mixing of the two individual components results in negligible attachment. Thus, the presence of surface nanobubbles under condition C might be a vital factor for the higher A_a value.

It should be noted that large bubbles could adhere to hydrophilic particles, while it would be complicated for bulk nanobubbles to adsorb on the hydrophilic particle surface. This contradictory phenomenon originated from the differences in the interaction mechanisms. The attachment between large bubbles and hydrophilic particles included various processes, from the free-rise of a small, clean single bubble, to the collision [49]. However, bulk nanobubbles could be stable, and their state of motion would be Brownian motion according to the stability mechanism of bulk nanobubbles [52]. The motion state of bulk nanobubbles indicated that bulk nanobubbles might not receive enough opportunities to contact with particles. In addition, large bubbles had enough energy to overcome the viscous resistance and collide, attaching with particles during its rising process compared to bulk nanobubbles.

5. Conclusions

Exploring the effect of roughness and nanobubble on particle-conventional air bubble attachment indicated that although the temperature rise method generated nanobubbles on the surface of hydrophilic smooth and rough glass beads, it showed little impact on the attachment of hydrophilic glass beads to the bubble surface. The overall increase of attachment area (A_a) induced by nanobubbles was less than 1%, contributing to the unstable nature of the nanobubbles formed on the hydrophilic surface. Rough glass bead particles attached more strongly to the bubble surface than the smooth glass beads. In other words, bubble = particle attachment could be improved by increasing the particle roughness. This enhancement would be because rough glass beads had a wider contact area with the bubbles, hence attached more easily.

Author contributions

Shaoqi Zhou: methodology, software, validation, formal analysis, investigation, writing - original draft; **Xiangning Bu**: conceptualization, resources, data curation, writing - original draft, writing - review & editing, visualization, supervision, project administration, funding acquisition; **Xuexia Wang**: formal analysis and investigation; **Chao Ni**: methodology, funding acquisition, and software; **Guangxi Ma**: methodology, software, and validation; **Yujin Sun**: methodology and software; **Guangyuan Xie**: resources, **Muidh Alheshibri**: funding acquisition, writing - original draft, and writing - review & editing; **Muhammad Bilal**: conceptualization, writing - original draft, and writing - review & editing; **Ahmad Hassanzadeh**: writing – interpretation of data, original draft and writing - review & editing. **Saeed Chehreh Chelgani**: interpretation of

data, validating, advising, editing & writing-original draft and revised version.

Funding

The authors gratefully acknowledge financial support from the National Natural Science Foundation of China (Grant No.51904296) and the Science Foundation for Youths of Shanxi Province (201901D211039). MA extends his appreciation to the Deputyship for Research & Innovation, Ministry of Education in Saudi Arabia, for funding his research work through the project number IF-2020-022-Sci at Imam Abdulrahman bin Faisal University. Additionally, we would like to thank the anonymous reviewers for their insightful remarks, constructive comments, and fruitful criticisms.

Declaration of Competing Interest

The authors declare that they have no known competing financial interests or personal relationships that could have appeared to influence the work reported in this paper.

REFERENCES

[1] Fan X, Zhang Z, Li G, Rowson N. Attachment of solid particles to air bubbles in surfactant-free aqueous solutions. Chem Eng Sci 2004;59:2639–45.
[2] Hassanzadeh A, Firouzi M, Albijanic B, Celik MS. A review on determination of particle–bubble encounter using analytical, experimental and numerical methods. Minerals Eng 2018;122:296–311.
[3] Bu X, Chen Y, Ma G, Sun Y, Ni C, Xie G. Differences in dry and wet grinding with a high solid concentration of coking coal using a laboratory conical ball mill: breakage rate, morphological characterization, and induction time. Adv Powder Technol 2019;30:2703–11.
[4] Guven O, Kaymakoğlu B, Ehsani A, Hassanzadeh A, Sivrikaya O. Effects of grinding time on morphology and collectorless flotation of coal particles. Powder Technol 2021:117010.
[5] Xing Y, Zhang Y, Ding S, Zheng X, Xu M, Cao Y, et al. Effect of surface roughness on the detachment between bubble and glass beads with different contact angles. Powder Technol 2020;361:812–6.
[6] Wang X, Zhang Q. Role of surface roughness in the wettability, surface energy and flotation kinetics of calcite. Powder Technol 2020;371:55–63.
[7] Hassanzadeh A, Azizi A, Kouachi S, Karimi M, Celik MS. Estimation of flotation rate constant and particle-bubble interactions considering key hydrodynamic parameters and their interrelations. Minerals Eng 2019;141:105836.
[8] Pushkarova R, Horn R. Bubble-solid interactions in water and electrolyte solutions. Langmuir 2008;24(16):8726–34. the ACS journal of surfaces and colloids.
[9] Hassanzadeh A, Kouachi S, Hasanzadeh M, Çelik MS. A new insight to the role of bubble properties on inertial effect in particle bubble interaction. J Dispersion Sci Technol 2017;38:953–60.
[10] Krasowska M, MbBysa K, Beattie D. Recent advances in studies of bubble-solid interactions and wetting film stability. Curr Opin Colloid Interface Sci 2019;44:48–58.
[11] Sun Y, Li Y, Dong X, Bu X, Drelich JW. Spreading and adhesion forces for water droplets on methylated glass surfaces. Colloids Surf A Physicochem Eng Asp 2020;591:124562.
[12] Nguyen A, Evans G, Nalaskowski J, Miller JD. Hydrodynamic interaction between an air bubble and a particle: atomic force microscopy measurements. Exp Therm Fluid Sci 2004;28:387–94.
[13] Xing Y, Gui X, Cao Y. The hydrophobic force for bubble-particle attachment in flotation - a brief review. Phys Chem Chem Phys 2017;36:24421–35. Phys Chem Chem Phys.
[14] Uddin S, Li Y, Mirnezami M, Finch J. Effect of particles on the electrical charge of gas bubbles in flotation. Minerals Eng 2012;36:160–7.
[15] Wu C, Wang L, Harbottle D, Masliyah J, Xu Z. Studying bubble–particle interactions by zeta potential distribution analysis. J Colloid Interface Sci 2015;449:399–408.
[16] Derjaguin B, Landau L. Theory of the stability of strongly charged lyophobic sols and of the adhesion of strongly charged particles in solutions of electrolytes. Prog Surf Sci 1941;43:30–59.
[17] Hassas BV, Caliskan H, Guven O, Karakas F, Cinar M, Celik MS. Effect of roughness and shape factor on flotation characteristics of glass beads. Colloids Surf A Physicochem Eng Asp 2016;492:88–99.
[18] Guven O, Ozdemir O, Karaagaclioglu IE, Çelik MS. Surface morphologies and floatability of sand-blasted quartz particles. Minerals Eng 2015;70:1–7.
[19] Wang D, Zhu Z, Yang B, Yin W, Drelich J. Nano-scaled roughness effect on air bubble-hydrophilic surface adhesive strength. Colloids Surf A Physicochem Eng Asp 2020;603:125228.
[20] Sygusch J, Rudolph M. A contribution to wettability and wetting characterisation of ultrafine particles with varying shape and degree of hydrophobization. Appl Surf Sci 2021;566(3):150725.
[21] Wu Z, Zhang X, Zhang X-d, Li G, Sun J-l, Zhang Y, et al. Nanobubbles influence on BSA adsorption on mica surface. Surf Interface Anal 2006;38:990–5.
[22] Pan G, Yang B. Effect of surface hydrophobicity on the formation and stability of oxygen nanobubbles. Phys Chem Phys Chem 2012;13(8):2205–12. a European journal of chemical physics and physical chemistry.
[23] Maheshwari S, vanKruijsdijk C, Sanyal S, Harvey A. Nucleation and growth of a nanobubble on rough surfaces. Langmuir 2020;36(15):4108–15.
[24] Stöckelhuber KW, Radoev B, Wenger A, Schulzet HJ. Rupture of wetting films caused by nanobubbles. Langmuir 2012;20(1):164–8.
[25] Zhou ZA, Xu Z, Finch JA, Masliyah JH, Chow RS. On the role of cavitation in particle collection in flotation-A critical review. II. Minerals Eng 2009;22(5):419–33.
[26] Zhang F, Sun L, Yang H, Gui X, Schönherr H, Kappl M, et al. Recent advances for understanding the role of nanobubbles in particles flotation. Adv Colloid Interface Sci 2021;291:102403.
[27] Zhou S, Wang X, Bu X, Wang M, An B, Shao H, et al. A novel flotation technique combining carrier flotation and cavitation bubbles to enhance separation efficiency of ultra-fine particles. Ultrason Sonochem 2020;64:105005.
[28] Lei W, Zhang M, Zhang Z, Zhan N, Fan R. Effect of bulk nanobubbles on the entrainment of kaolinite particles in flotation. Powder Technol 2020;362:84–9.
[29] Dang Vu T, Hupka J, Drzymala J. Impact of roughness on hydrophobicity of particles measured by the Washburn method. Physicochem Probl Miner Process 2006;56(5):818–28.
[30] Guven O, Karakb F, Kodrazi N, Çelik M. Dependence of morphology on anionic flotation of alumina. Int J Miner Process 2016;156:69–74.

[31] Wang S, Fan H, He H, Tang L, Tao X. Effect of particle shape and roughness on the hydrophobicity of low-rank coal surface. Int J Coal Prep Util 2020;40:876–91.
[32] Li Z, Rao F, Corona-Arroyo M, Bedolla-Jacuinde A, Song S. Comminution effect on surface roughness and flotation behavior of malachite particles. Minerals Eng 2019;132:1–7.
[33] Guven O, Celik MS, Drelich JW. Flotation of methylated roughened glass particles and analysis of particle–bubble energy barrier. Minerals Eng 2015;79:125–32.
[34] Li Y, Wu F, Xia W, Mao Y, Peng Y, Xie G. The bridging action of microbubbles in particle-bubble adhesion. Powder Technol 2020;375:271–4.
[35] Bu X, Zhang T, Chen Y, Xie G, Peng Y. Comparative study of conventional cell and cyclonic microbubble flotation column for upgrading a difficult-to-float Chinese coking coal using statistical evaluation. Int J Coal Prep Util 2020;40(6):359–75.
[36] Ke S, Xiao W, Quan N, Dong Y, Zhang L, Hu J. Formation and stability of bulk nanobubbles in different solutions. Langmuir 2019;35(15):5250–6. the ACS journal of surfaces and colloids.
[37] Najafi AS, Drelich J, Yeung A, Xu Z, Masliyah J. A novel method of measuring electrophoretic mobility of gas bubbles. J Colloid Interface Sci 2007;308(2):344–50.
[38] Yang H, Xing Y, Sun L, Cao Y, Gui X. Kinetics of bubble-particle attachment and detachment at a single-bubble scale. Powder Technol 2020;370:251–8.
[39] Bu X, Xie G-y, Peng Y-l, Ge L, Ni C. Kinetics of flotation. Order of process, rate constant distribution and ultimate recovery. Physicochem Probl Miner Process 2016;53:342–65.
[40] Rezai B, Rahimi M, Aslani MR, Eslamian A, Dehghani F. Relationship between surface roughness of minerals and their flotation kinetics. In: Proceedings of the XI international seminar on mineral processing Technology (MPT-2010). India: CSIR-National Metallurgical Laboratory, NML Jamshedpur; 2010.
[41] Bu X, Xie G-y, Chen Y, Ni C. The order of kinetic models in coal fines flotation. Int J Coal Prep Util 2017;37:113–23.
[42] Bu X, Wang X, Zhou S, Li B, Zhan H, Xie G-y. Discrimination of six flotation kinetic models used in the conventional flotation and carrier flotation of - 74 μm coal fines. ACS Omega 2020;5:13813–21.
[43] Marion C, Jordens A, Li R, Rudolph M, Waters K. An evaluation of hydroxamate collectors for malachite flotation. Separ Purif Technol 2017;183:258–69.
[44] Oney O, Samanli S, Çelik H, Tayyar N. Optimization of operating parameters for flotation of fine coal using a box-behnken design. Int J Coal Prep Util 2015;35:233–46.
[45] Xu M. Modified flotation rate constant and selectivity index. Minerals Eng 1998;11:271–8.
[46] Yin Z-g, Xu L, He J, Wu H, Fang S, Khoso SA, et al. Evaluation of l-cysteine as an eco-friendly depressant for the selective separation of MoS_2 from PbS by flotation. J Mol Liq 2019;282:177–86.
[47] Zhou S, Xuexia W, Bu X, Shao H, Hu Y, Alheshibri M, et al. Effects of emulsified kerosene nanodroplets on the entrainment of gangue materials and selectivity index in aphanitic graphite flotation. Minerals Eng 2020;158:106592.
[48] Jiang L, Krasowska M, Fornasiero D, Koh P, Ralston J. Electrostatic attraction between a hydrophilic solid and a bubble. Phys Chem Chem Phys 2010;12(43):14527–33.
[49] Parkinson L, Ralston J. Dynamic aspects of small bubble and hydrophilic solid encounters. Adv Colloid Interface Sci 2011;168(1):198–209.
[50] Ha KS, Sun PH, Donggun K, Hwan KM. Wetting characteristic of bubble on micro-pillar structured surface under a water pool. Exp Therm Fluid Sci 2018;100:135–43.
[51] An H, Tan BH, Zeng Q, Ohl C-D. Stability of nanobubbles formed at the interface between cold water and hot highly oriented pyrolytic graphite. Langmuir 2016;32(43):11212–20.
[52] Alheshibri M, Qian J, Jehannin M, Craig VSJ. A history of nanobubbles. Langmuir 2016;32(43):11086–100.
[53] Sun Y, Xie G, Peng Y, Xia W, Sha J. Stability theories of nanobubbles at solid–liquid interface: a review. Colloids Surf A Physicochem Eng Asp 2016;495:176–86.
[54] Fang Z, Wang X, Zhou L, Zhang L, Hu J. Formation and stability of bulk nanobubbles by vibration. Langmuir 2020;36(9):2264–70.
[55] Zhou S, Nazari S, Hassanzadeh A, Bu X, Ni C, Peng Y, et al. The effect of preparation time and aeration rate on the properties of bulk micro-nanobubble water using hydrodynamic cavitation. Ultrason Sonochem 2022;84:105965.